



## A new species of *Neblinaphryne* (Anura: Brachycephaloidea: *Neblinaphrynidae*) from Serra do Imeri, Amazonas state, Brazil



ANTOINE FOUQUET<sup>1\*</sup>, LEANDRO J.C.L. MORAES<sup>2</sup>, TARAN GRANT<sup>2</sup>, RENATO RECODER<sup>2</sup>, AGUSTÍN CAMACHO<sup>3</sup>, JOSÉ MÁRIO GHELLERE<sup>2</sup>, ALEXANDRE BARUTEL<sup>1</sup> & MIGUEL TREFAUT RODRIGUES<sup>2</sup>

<sup>1</sup>Centre de Recherche sur la Biodiversité et l'Environnement (CRBE), UMR 5300 CNRS-IRD-TINP-UT3, Université Toulouse III – Paul Sabatier, Bât. 4R1, 118 route de Narbonne, 31062 Toulouse cedex 9, France.

 <https://orcid.org/0000-0003-4060-0281>;  <https://orcid.org/0009-0002-0897-7425>

<sup>2</sup>Universidade de São Paulo, Instituto de Biociências, Departamento de Zoologia, São Paulo, SP, Brazil.

 <https://orcid.org/0000-0001-6704-898X>;  <https://orcid.org/0000-0003-1726-999X>;

 <https://orcid.org/0000-0001-9931-9238>;  <https://orcid.org/0000-0003-3958-9919>

<sup>3</sup>Universidad Autónoma de Madrid. Facultad de Ciencias (Edificio Biología). C. Darwin, 2, Fuencarral-El Pardo, 28049, Madrid.

 <https://orcid.org/0000-0003-2978-792X>

\*Corresponding author:  [fouquet.antoine@gmail.com](mailto:fouquet.antoine@gmail.com)

### Abstract

The highlands of the Guiana Shield (Pantepui) in northern South America harbor a unique fauna and flora. However, this diversity remains poorly documented, as many Pantepui massifs remain little explored or unexplored, mainly because their access is very challenging. Considering amphibians, 11 genera are endemic or sub-endemic to Pantepui, and one of them, *Neblinaphryne*, is monospecific and was recently described from the Neblina massif, at the border between Brazil and Venezuela. We recently undertook an expedition in the nearby, previously uninventoried Imeri massif and discovered a new species of this genus. We describe this new species herein as *Neblinaphryne imeri* **sp. nov.**, combining molecular, external morphological, acoustic, osteological and myological data. The new species shares with the other *Neblinaphryne* species (*N. mayeri*) minuscule septomaxillae and pointed terminal phalanges, confirming the morphological diagnostic characters of the genus. Nevertheless, the new species can promptly be distinguished from *N. mayeri* by having the head wider than long, a distinct color pattern, and prominent tubercles on the eyelid and humeral region, as well as osteological and genetic differences. These two species are likely endemic to their respective massifs, providing a striking new example of speciation by isolation within Pantepui, which was possibly mediated by climate and elevation, as previously hypothesized for many other lineages endemic to this region.

**Key words:** Amazonia, Amphibian, Biodiversity, Frog, Guiana Shield, Pantepui, Taxonomy, Systematics

### Introduction

The Pantepui region, the highlands of the Guiana Shield, consist of either peculiar sandstone table mountains or granitic massifs on which the sandstone layer has been weathered (Rull *et al.* 2019). These massifs frequently reach >2,000 m elevation and are scattered across southern Venezuela and adjacent Brazil and Guyana. They are surrounded by upland forests and savannas with Amazonian affinities in terms of species composition and species phylogenetic relatedness (Kok 2013; Rull & Vegas-Vilarrúbia 2020). Unlike the lower surroundings, the highlands host many ancient lineages of amphibians, as the endemic genera *Oreophrynella*, *Minyobates*, *Nesorohyla*, *Myersiophyla* and *Ceuthomantis*, and the near-endemic *Stefania* and *Tepuihyla* (Heinicke *et al.* 2009; Santos *et al.* 2009; Kok 2013; Kok *et al.* 2017; 2018; Pinheiro *et al.* 2019; Ortiz *et al.* 2022). There are also many endemic squamate genera such as *Adercosaurus*, *Kaieatusaurus*, *Paikwaophis*, *Pantepuisaurus*, *Riolama* and *Yanomamia* (Myers & Donnelly 2001; Kok 2005; 2009; 2015; Pellegrino *et al.* 2018; Recoder *et al.* 2020; Kok & Means 2023), as well as endemic species of birds (e.g., Mayr & Phelps 1967), mammals (e.g., Leite *et al.* 2015), invertebrates (e.g., Kok *et al.* 2019), and plants (e.g., Steyermark 1986; Berry & Riina 2005).

There are two recent additions to the list of ancient amphibian lineages endemic to Pantepui with *Neblinaphryne mayeri* and *Caligophryne doylei* (Fouquet *et al.* 2024). These two additions were remarkable because they also required two new genera and two new families to be recognized and also because they were found in sympatry on the Neblina massif, located in the southwestern part of Pantepui, at the border between Brazil and Venezuela. Like most Pantepui endemic frogs, these two new lineages diverged from their closest relatives before the Neogene and are striking reminders of how fragmentary our understanding is of the actual diversity that Pantepui may harbor.

To fill some of these gaps, we undertook a multidisciplinary scientific expedition supported by the Brazilian Army in Serra do Imeri, near the Neblina massif, and found a new species of frog related to *N. mayeri*. We herein name and describe this new species.

## Materials and Methods

### Study area and species sampling

Serra do Imeri is a highly eroded granitic massif of the Precambrian basement of the Guiana Shield, situated at the southern border of Pantepui. This highly dissected block of mountains extends for ca. 50 km along the northern part of the state of Amazonas, near the Brazil–Venezuela border. The part of this massif above 1,500 m is isolated from the Neblina massif on the west by the Cauaburis River valley, corresponding to a minimum stretch of ca. 20 km of lowlands (Fig. 1). On the northwest, massifs reaching >1,500 m are scattered along the border between the two countries and further extending southward within Brazil to the Tapirapecó mountains. However, long distances isolate the complex formed by these three southern massifs from other Pantepui highlands. Contrary to the Neblina massif where the Precambrian basement is covered by the sediments of the Roraima Formation, forming a plateau exceeding 2,000 m asl, there is no plateau at Serra do Imeri. Its relief is highly rugged and eroded and the Precambrian basement is frequently exposed.

Serra do Imeri's highest point, Pico do Imeri (Imeri peak), culminates at ca. 2,240 m. It is surrounded by lowlands covered by Amazonian forest, which reaches ca. 1,000 m and is gradually replaced by montane forest up to an elevation of ca. 1,800 m. Above this elevation, montane forests progressively give space to scrublands with scattered trees and meadows on peat and extensive bogs with giant bromeliads (Fig. 2). The massif lies within the Brazilian protected area Parque Nacional do Pico da Neblina, which overlaps Yanomami territory and was virtually unexplored before our expedition. Our camp was set up by the Brazilian Army on the slope facing the Pico do Imeri (geographic coordinates: 0.470833 N, 65.33889 W). The local vegetation is dominated by low- to mid-size shrubs and meadows where Bromeliaceae (especially *Brocchinia tatei*), Rapateaceae, Xyridaceae, and Theaceae are abundant in wet peat. Lower parts of the slopes are covered by low canopy forest.

We undertook fieldwork from 8 to 17 November 2022. Although we installed pitfalls consisting of 22 sets of Y-shaped 20 L buckets (four buckets per Y) connected to the central one by 4-m fences, the results were unsuccessful for the present species, which were all hand-captured. Specimens were euthanized with an intraperitoneal injection of lidocaine hydrochloride. We then obtained tissue samples (liver or muscle pieces preserved in 95% ethanol) from all individuals. These tissue samples were later deposited under their original field numbers (MTR series) at the tissue collection of the Department of Zoology, Instituto de Biociências, Universidade de São Paulo, Brazil. Following tissue sampling, specimens were fixed in 10% formalin and then transferred to 70% ethanol for permanent storage. Voucher specimens were deposited in the Herpetological Collection of Museu de Zoologia, Universidade de São Paulo (MZUSP), keeping their original field tags for future reference.

### Molecular survey and phylogenetic analyses

We produced a 1,570 base pairs (bp) long sequence of 16S rDNA, and a 672 bp long sequence of cytochrome oxidase I (COI) from one sample of the new species (MZUSP 160476/MTR 30964). Newly generated sequences (GenBank accessions 16S: PP789109, COI: PP788591) were obtained after extraction of the genomic DNA from tissue samples (muscle or liver) using either the Wizard® Genomic DNA Purification Kit (Promega; Madison, WI, USA) or the DNeasy® Blood & Tissue Kit (Qiagen; Hilden, Germany) following the manufacturer's protocols, amplification of the targeted loci by standard PCR protocols and sequencing by Sanger reactions (Appendix 1 for primers).



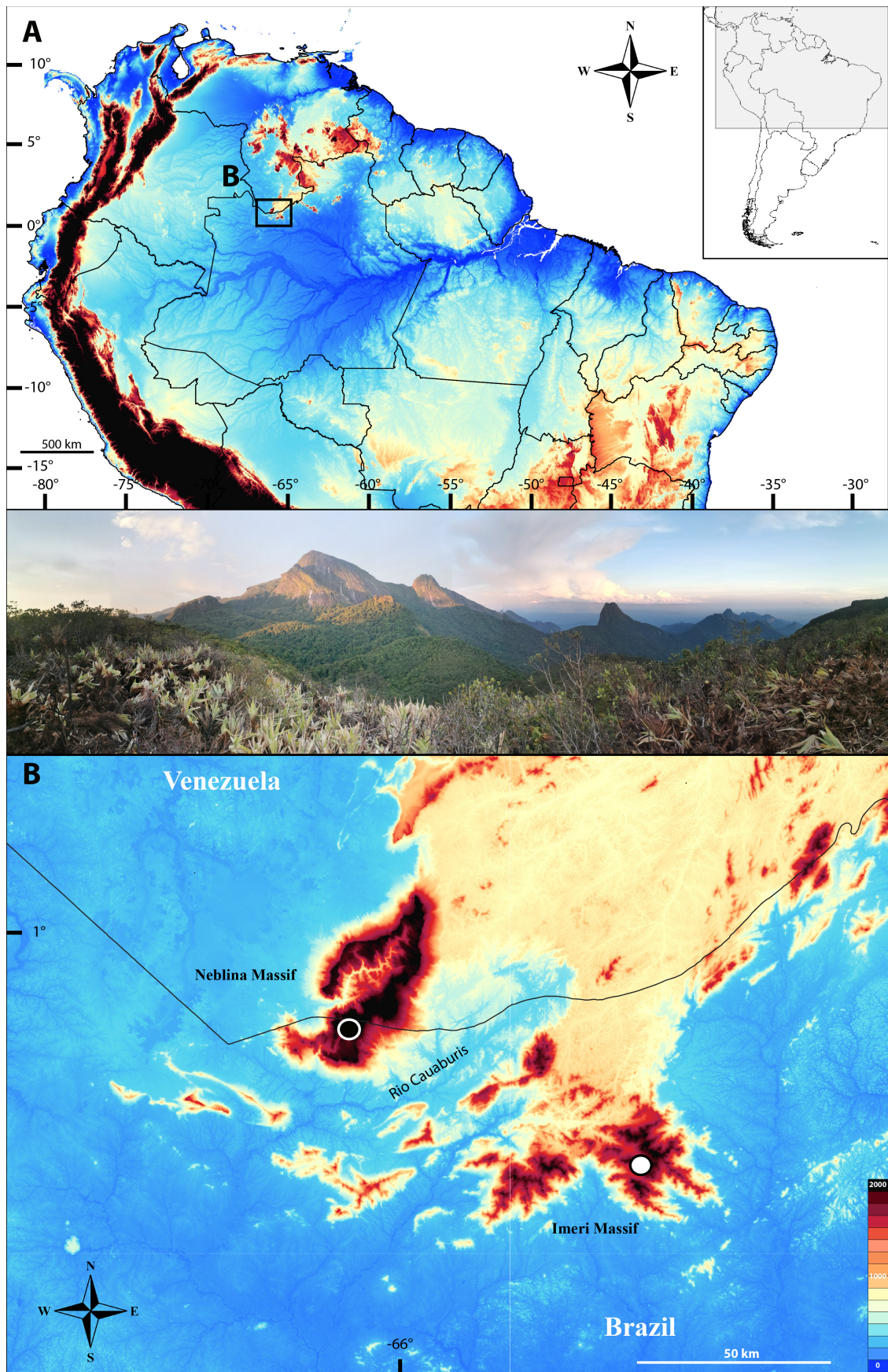


**FIGURE 1.** Topographic maps of (A) northern South America, (B) southern Pantepui, highlighting the neighboring Neblina and Imeri massifs. The white circle represents the type locality of *Neblinaphryne mayeri* and the white filled dot the one of *N. imeri* sp. nov. The landscape image depicts the panoramic view of the sampled area of the Serra do Imeri, with the Imeri peak in the background (the highest on the left).





**FIGURE 2.** Four pictures taken on Serra do Imeri (Amazonas, Brazil) illustrating both open (giant bromeliads, top left) and mountain forest (mossy, all other images) habitats where *Neblinaphryne imeri* **sp. nov.** has been heard calling and collected.

We undertook a preliminary Neighbour Joining analysis using Geneious 9 (<https://www.geneious.com>) to narrow down the phylogenetic affinities of the new species among the major families of Nobleobatrachia, because we were not certain of the generic identification. This analysis inferred a highest genetic similarity of the new species with *Neblinaphryne mayeri*, part of the superfamily Brachycephaloidea. Therefore, we collated our new sequences with available homologous sequences (downloaded from GenBank) of most genera of Brachycephaloidea (34 terminals) and most families of Nobleobatrachia (13 terminals). We caution that our taxon sampling was intended to test the placement of the new species and not to infer higher relationships among brachycephaloids and other Nobleobatrachia. The final matrix contained a total of 47 terminals (Appendix 2). The sequences were aligned using the MAFFT7 online server under default parameters except the E-INS-i strategy for the 16S, which is designed for sequences with multiple conserved domains and long gaps (Katoh *et al.* 2013) and considering the reading frame for COI, resulting in a final alignment of 2,243 base pairs (bp).

Using this dataset, we investigated the phylogenetic relationships among taxa under Maximum Likelihood (ML) in IQTREE2 (Minh *et al.* 2020), using a partitioned analysis (16S:1; Pos1COI:2; Pos2COI:3; Pos3COI:4)



as suggested by IQTREE2 ModelFinder (Kalyaanamoorthy *et al.* 2017). Tree search and standard nonparametric bootstrapping values (Felsenstein 1985) were estimated using 1,000 pseudoreplicates. The tree was rooted on *Rhinoderma darwinii* (Rhinodermatidae).

### Morphological analyses

We examined 10 specimens of the new species, seven males and three females. We mainly followed Lynch & Duellman (1997) and Duellman & Lehr (2009) for diagnosis and descriptions, with modifications. Sex was determined by the presence of vocal slits and direct inspection of oocytes through the ventral skin in females in life. The gonads of two specimens (MZUSP 160478 / MTR 30990 adult male; MZUSP 160472 / MTR 30864 adult female) were examined after lateral abdominal incisions. We took the following measurements using calibrated dorsal and ventral pictures of the specimens via Image J (Rueden *et al.*, 2017) to the nearest 0.01 mm: SVL, snout–vent length; HL, head length (from the posterior margin of lower jaw to tip of snout); HW, head width (measured at the level of the rictus); IND, internarial distance; END, eye to nostril distance; ED, eye diameter (measured horizontally); IOD, interorbital distance (taken between the anterior corners of the eyes); UEW, upper eyelid width (maximum width dorsally); TD, tympanum diameter (measured horizontally); ARM, arm length (from the posterior margin of the thenar tubercle to the elbow); HAN, hand length (from the posterior margin of the thenar tubercle to the tip of the Finger III); TH, thigh length (from vent to flexed knee); TL, tibia length (from flexed knee to flexed ankle); TAL, tarsal length (from flexed ankle to inner metatarsal tubercle); FTL, foot length (from the proximal border of the inner metatarsal tubercle to the tip of the fourth toe). We rounded all measurements to one decimal to avoid pseudo-precision. We also measured the length of Fingers I and II from the posterior margin of the thenar tubercle to the tip of the fingers and of Toes III and V from the proximal border of the inner metatarsal tubercle to the tip of the toes. Measurements are reported as the mean  $\pm$  standard deviation (minimum–maximum).

### Osteology and musculature

Three specimens of the new species were  $\mu$ CT-scanned (kV = 40–70, resolution < 20  $\mu$ m) using a Bruker Skyscan 1176 at the Universidade de São Paulo, Brazil. Volume renderings of the full skeleton of the specimens (MZUSP 160478/MTR 30990; MZUSP 160474/MTR 30895; MZUSP 160473/MTR 30892) was obtained using Avizo (FEI Visualization Sciences Group, Burlington, MA, USA).  $\mu$ CT-scans have been deposited in MorphoSource (accessions: 000628931, 000628940, 000629011). We compared the osteology of the new species with the one of *N. mayeri* (accessions: 000554956, 000554966).

We examined myological characters related to the insertion of the *m. iliacus externus* and the *m. tensor fasciae latae*, two muscles originating on the iliac shaft. These muscles present extensive variation in frogs (Dunlap 1960) and certain states have been suggested to represent synapomorphies for some clades of Brachycephaloidea (Ospina-Sarria & Grant 2022). For this purpose, we made a lateral incision in the skin of an individual of the new species (MZUSP 160477/MTR 30988) to expose the superficial pelvic and thigh muscles. The attachment of the muscles was observed under a stereomicroscope. Terminology follows Dunlap (1960) and Ospina-Sarria & Grant (2022).

### Bioacoustics

We recorded the advertisement calls of four males (MZUSP 160479/MTR 30991 and three uncollected individuals) of the new species calling at dusk (15–16°C taken on the ground of the forest litter). They consist of two types of notes. Type 1 notes consist of a long series of pulses with downward frequency and amplitude followed by a series of shorter pulsed notes (Type 2 notes). We thus considered the calls as clusters of these notes and analyzed the two types of notes independently following a call-centered definition (Köhler *et al.* 2017). We measured the following 10 temporal variables (a single recording per calling male; averaged when several measures could be taken) using Audacity v.2.1.1: call length (CL), Type 1 note length (NL1); Type 2 individual note length (NL2), silence between note 1 & 2 (SN1); silence between note 2 and 3 (SN2); number of pulses in Type 1 note (NP1); number of pulses in Type 2 notes (NP2); silence between the two first pulses of Type 1 notes (SPs); silence between the two last pulses of Type 1 notes (SPe); and four spectral variables: fundamental frequency at the beginning (first 0.1 s window) of the Type 1 notes (FFs); fundamental frequency at the end (last 0.1 s window) of the Type 1 notes (FFe); dominant frequency at the beginning (first 0.1 s window) of the Type 1 notes (DFs); dominant frequency at the end (last 0.1 s window) of the Type 1 notes (DFe); dominant frequency of Type 2 notes (taken on the entire note length). Recordings have been deposited at sonothèque.mnhn.fr (accessions: MNHN-SO-2024-2983–6).

## Phylogenetic analyses

Phylogenetic tree showing relationships among various species, with bootstrap values indicated at the nodes. The tree is rooted at the bottom with *Rhinoderma darwini*. Major clades are labeled on the right: Strabomantidae, Caligophrynidae, Brachycephalidae, Craugastoridae, Eleutherodactylidae, and Other Hyloidea. A scale bar of 0.4 is shown at the top left.

Species listed (from top to bottom):

- Pristimantis koehleri*
- Pristimantis gutturalis*
- Pristimantis skydmainos*
- Pristimantis curtipes*
- Pristimantis lanthanites*
- Pristimantis aff. pluvialis*
- Pristimantis galdi*
- Pristimantis diadematus*
- Pristimantis espedeus*
- Phynopus horstpauli*
- Oreobates quixiensis*
- Niceforonia brunnea*
- Holoaden luederwaldti*
- Bryophryne bustamantei*
- Noblella myrmecoides*
- Strabomantis sulcatus*
- Caligophryne doylei*
- Brachycephalus quiririensis*
- Brachycephalus pulex*
- Tachiramantis lentiginosus*
- Serranobatrachus sanctaemartae*
- Ischnocnema erythromera*
- Ischnocnema henselii*
- Adelophryne gutturosa*
- Adelophryne baturitensis*
- Phyzelaphryne miriamae*
- Haddadus binotatus*
- Diasporus sp.*
- Eleutherodactylus atkinsi*
- Craugastor raniformis*
- Craugastor augusti*
- Ceuthomantis sp. Neblina*
- Neblinaphryne imeri sp. nov. MZUSP160476 (MTR30964)*
- Neblinaphryne mayeri*
- Pseudis tocantins*
- Dendropsophus ebraccatus*
- Pleurodema thaul*
- Ceratophrys ornata*
- Hyalinobatrachium fleischmanni*
- Odontophrynus occidentalis*
- Telmatobius bolivianus*
- Hylodes meridionalis*
- Gastrotheca pseustes*
- Cryptobatrachus fuhrmanni*
- Eupsophus vertebralis*
- Phyllobates terribilis*
- Rhinoderma darwini*

Clade labels on the right:

- Strabomantidae
- Caligophrynidae
- Brachycephalidae
- Craugastoridae
- Brachycephalidae
- Eleutherodactylidae
- Craugastoridae
- Eleutherodactylidae
- Craugastoridae
- Ceuthomantidae
- Neblinaphrynidae
- Other Hyloidea

78 · Zootaxa 5514 (1) © 2024 Magnolia Press



## Phenotypic data

Morphometric variation is summarized in Table 1 and qualitative morphological characters (integumental, osteological, and myological) are illustrated in Figs. 4–7. Acoustic measurements are summarized in Table 2 and a graphic representation of an advertisement call is illustrated in Fig. 8. To avoid repetition, we restrict detailed phenotypic descriptions to the Taxonomy section.

**TABLE 1.** Body measurements of the type series of *Neblinaphryne imeri* sp. nov. compared to *N. mayeri*. Values presented in millimeters as mean  $\pm$  standard deviation (range, as minimum–maximum values).

	<i>Neblinaphryne imeri</i> sp. nov.		<i>Neblinaphryne mayeri</i>	
	Males $n=7$	Females $n=3$	Males $n=15$	Females $n=17$
<b>Snout–vent length (SVL)</b>	15.9 $\pm$ 1.1 (14.2–17.2)	19.8 $\pm$ 0.5 (19.2–20.1)	16.7 $\pm$ 1.9 (14.0–19.2)	18.1 $\pm$ 0.9 (15.9–20.1)
<b>Head length (HL)</b>	4.6 $\pm$ 0.4 (3.9–5.3)	5.6 $\pm$ 0.5 (5.1–6.0)	6.2 $\pm$ 0.9 (4.9–7.7)	6.6 $\pm$ 0.6 (5.7–7.5)
<b>Head width (HW)</b>	5.4 $\pm$ 0.4 (4.8–5.9)	6.8 $\pm$ 0.5 (6.3–7.2)	6.0 $\pm$ 0.8 (4.9–7.2)	6.4 $\pm$ 0.5 (5.5–7.3)
<b>Internarial distance (IND)</b>	1.9 $\pm$ 0.2 (1.6–2.0)	2.2 $\pm$ 0.2 (2.2–2.3)	1.9 $\pm$ 0.2 (1.5–2.3)	2.1 $\pm$ 0.1 (1.9–2.4)
<b>Eye to nostril distance (END)</b>	1.2 $\pm$ 0.1 (1.0–1.4)	1.4 $\pm$ 0.1 (1.3–1.6)	1.1 $\pm$ 0.2 (0.7–1.3)	1.3 $\pm$ 0.1 (1.1–1.4)
<b>Eye diameter (ED)</b>	2.0 $\pm$ 0.1 (1.8–2.2)	2.3 $\pm$ 0.2 (2.2–2.5)	2.1 $\pm$ 0.2 (1.9–2.5)	2.2 $\pm$ 0.2 (2.0–2.5)
<b>Interorbital distance (IOD)</b>	1.7 $\pm$ 0.2 (1.6–2.2)	2.2 $\pm$ 0.2 (2.0–2.4)	1.7 $\pm$ 0.2 (1.2–2.1)	2.1 $\pm$ 0.2 (1.7–2.3)
<b>Upper eyelid width (UEW)</b>	1.2 $\pm$ 0.2 (1.0–1.4)	1.4 $\pm$ 0.1 (1.3–1.4)	1.3 $\pm$ 0.1 (1.2–1.5)	1.4 $\pm$ 0.1 (1.2–1.5)
<b>Arm length (ARM)</b>	3.9 $\pm$ 0.3 (3.5–4.4)	4.9 $\pm$ 0.6 (4.2–5.4)	4.2 $\pm$ 0.4 (3.3–4.8)	4.5 $\pm$ 0.2 (4.1–5.0)
<b>Hand length (HAN)</b>	3.3 $\pm$ 0.4 (2.8–3.9)	4.0 $\pm$ 0.1 (3.9–4.1)	3.8 $\pm$ 0.5 (2.9–4.5)	4.0 $\pm$ 0.2 (3.7–4.3)
<b>Thigh length (TH)</b>	7.8 $\pm$ 0.4 (7.5–8.5)	9.0 $\pm$ 0.8 (8.0–9.5)	7.5 $\pm$ 0.8 (6.0–9.0)	8.2 $\pm$ 0.3 (7.6–8.8)
<b>Tibia length (TL)</b>	7.2 $\pm$ 0.4 (6.6–7.8)	8.6 $\pm$ 0.5 (8.0–8.9)	7.1 $\pm$ 0.7 (5.6–8.0)	7.6 $\pm$ 0.3 (7.0–8.1)
<b>Tarsal length (TAL)</b>	4.8 $\pm$ 0.3 (4.2–5.3)	5.3 $\pm$ 0.5 (4.8–5.7)	5.3 $\pm$ 0.5 (4.1–6.1)	5.6 $\pm$ 0.3 (5.1–6.0)
<b>Foot length (FTL)</b>	7.3 $\pm$ 0.6 (6.6–8.2)	8.3 $\pm$ 0.3 (8.0–8.5)	7.9 $\pm$ 0.7 (6.7–9.0)	8.2 $\pm$ 0.4 (7.5–9.2)
<b>Finger I length (FI)</b>	2.0 $\pm$ 0.2 (1.6–2.3)	2.3 $\pm$ 0.1 (2.2–2.4)		
<b>Finger II length (FII)</b>	2.2 $\pm$ 0.3 (1.8–2.7)	2.6 $\pm$ 0.2 (2.3–2.6)		
<b>Toe III length (TIII)</b>	4.7 $\pm$ 0.4 (4.0–5.3)	5.7 $\pm$ 0.3 (5.4–5.9)		
<b>Toe V length (TV)</b>	4.8 $\pm$ 0.4 (4.1–5.3)	5.6 $\pm$ 0.3 (5.3–5.9)		

## *Neblinaphryne imeri* sp. nov.

**Holotype (Fig. 4).** MZUSP 160479 (MTR 30991), an adult male from Serra do Imeri, Parque Nacional Pico da Neblina, Santa Isabel do Rio Negro, Amazonas state, Brazil (0.470833 N, 65.33889 W, ca. 1800 m elevation), collected 16 November 2022 by M.T. Rodrigues; A. Camacho; A. Fouquet; J.M.B. Ghellere; T. Grant; L. Moraes; R. Recoder.

**Paratopotypes ( $n = 9$ ) (Fig. 5).** MZUSP 160471 (MTR 30853), MZUSP 160474–160475, (MTR 30895, MTR 30928), MZUSP 160477–160478 (MTR 30988, MTR 30990), and MZUSP 160480 (MTR 31003), six adult males, and MZUSP 160476 (MTR 30964), MZUSP 160472–160473 (MTR 30864, MTR 30892), three adult females, all collected between 8 and 16 November 2022 by the same collectors.

**Etymology.** The specific epithet “*imeri*” is a noun in apposition and refers to the Imeri mountain massif where the species occurs.

**Generic placement.** The new species is assigned to the genus *Neblinaphryne* based on its phylogenetic relationship as assessed by molecular data (Fig. 3) and its pointed (not T-shaped) terminal phalanges and minuscule septomaxillae, two osteological characters that were identified as diagnostic of the genus by Fouquet *et al.* (2024).

**Definition.** A minute brachycephaloid frog characterized by: (1) SVL 15.9  $\pm$  1.1 mm in males, 19.8  $\pm$  0.5 mm in females (Table 1); (2) head wider than long, narrower than body; (3) tympanum indistinct, covered by skin and dorsally by a supratympanic fold, columella present (Fig. 6); (4) one prominent tubercle on each eyelid (cream-colored in life) and in the humeral region (white-tipped, Fig. 4); (5) frontoparietal smooth, cranial crests absent;



**FIGURE 4.** Holotype of *Neblinaphryne imeri* **sp. nov.** MZUSP 160479 (MTR 30991, adult male). (A) Dorsal and (B) ventral views in preservative; (C) palmar view of the left hand and (D) plantar view of the left foot; (E) dorsolateral and (F) ventral views in life. The humeral tubercle is indicated by white arrows on (A) and (E).





**FIGURE 5.** Dorsolateral and ventral views of paratypes of *Neblinaphryne imeri* **sp. nov.** in life. (A) MZUSP 160471 (MTR 30853); (B) MZUSP 160474 (MTR 30895); (C) MZUSP 160477 (MTR 30988); (D) MZUSP 160478 (MTR 30990); (E) MZUSP 160480 (MTR 31003); (F) MZUSP 160472 (MTR 30864); (G) MZUSP 160473 (MTR 30892); (H) MZUSP 160476 (MTR 30964).

(6) dentigerous process of vomer absent, vomers free of contact with any other bone; (7) subgular vocal sac, vocal slits present in males; (8) fingers fully developed without subarticular tubercles, finger tips not expanded, rounded on Finger I, pointed or mucronate on II and IV, mucronate on Finger III, without discs and circumferential grooves, terminal phalanges pointed; (9) outer metacarpal tubercle flat, drop-shaped, other tubercles on hands and fingers absent; (10) Finger I slightly shorter than Finger II; relative lengths of fingers:  $I < II < IV < III$ ; nuptial pads absent; (11) toes fully developed, toe tips not expanded, pointed or rounded on Toes I and V, mucronate on Toes II–IV, terminal phalanges pointed on Toes I and V and slightly knobbed on Toes II–IV; (12) relative lengths of toes:  $I < II < III < V < IV$ , Toe V only slightly longer than Toe III; (13) lateral fringes and webbing absent on fingers and toes; (14) toe subarticular tubercles absent; supernumerary tubercles absent; (15) outer metatarsal tubercle round, large, protruding, inner metatarsal tubercle ovoid, flat; (16) dorsolateral folds absent; (17) discoidal fold absent; (18) septomaxillae minuscule; (19) iris copper with dark reticulations in life, pupillary ring thin and often discontinuous, horizontal large and diffuse dark band and vertical thin, and sharp dark band reaching the pupil only on the lower portion; (20) *m. iliacus externus* originating via a single head anteriorly and extending in parallel alongside the entire length of the iliac shaft; (21) *m. tensor fasciae latae* originating anteriorly on the iliac shaft, immediately posterior to the sacral diapophyses (Fig. 7); (20) Testis immaculate white in males and oviduct expanded, convoluted and large white oocytes in females; (21) call consisting of long (414–592 ms) Type 1 notes formed by series of 31–70 pulses emitted with dominant frequency 3,010–3,957 Hz generally followed by shorter (76–180 ms) Type 2 notes that have otherwise the same basic structure (Fig. 8).

**Description of the holotype (Fig. 4).** Adult male with a ventral incision on the right side below the chest, SVL 16.3 mm, head slightly wider than long, head length 25% SVL; head width 38% SVL; snout short, rounded in dorsal and lateral views; upper eyelid width 62% of interorbital distance; eye to nostril distance 60% of eye diameter; nostrils ovoid. Pupil horizontal (Cervino *et al.* 2021). Tympanum indistinct, its dorsal portion concealed by a supra-

tympanic fold. Head without enlarged tubercles or folds except the two enlarged tubercles on each eyelid. Cranial crests and dentigerous processes of vomers absent. Vocal slits present, one on each side, from the jaw angle to the lateral base of the tongue; vocal sac subgular; tongue ovoid, free posteriorly for nearly half its length; choanae small, round, located laterally and anteriorly. Skin of dorsum, throat, and upper and lower limbs smooth with few small, scattered tubercles, notably on eyelids, dorsum, and legs; skin of belly finely granular. Prominent white-tipped tubercle present on the humeral region. Axillary membrane absent. Fingers without discs and circumferential grooves absent, tips unexpanded, rounded on Finger I, pointed on II and IV, mucronate on III; fingers lacking fringes and webbing. Finger I slightly shorter than Finger II; relative lengths of fingers  $I < II < IV < III$ . Outer metacarpal tubercle flat, drop-shaped; other tubercles on hand and fingers (e.g., subarticular, supernumerary) absent. Nuptial pads absent. Toes without discs and circumferential grooves, toe tips unexpanded, pointed on Toe I, mucronate on Toes II–IV, rounded on Toe V; toes lacking lateral fringes and webbing. Toe V slightly longer than Toe III; relative lengths of toes  $I < II < III < V < IV$ . Inner metatarsal tubercle ovoid, flat. Outer metatarsal tubercle rounded, prominent, slightly larger than inner one. Subarticular and supernumerary tubercles absent.

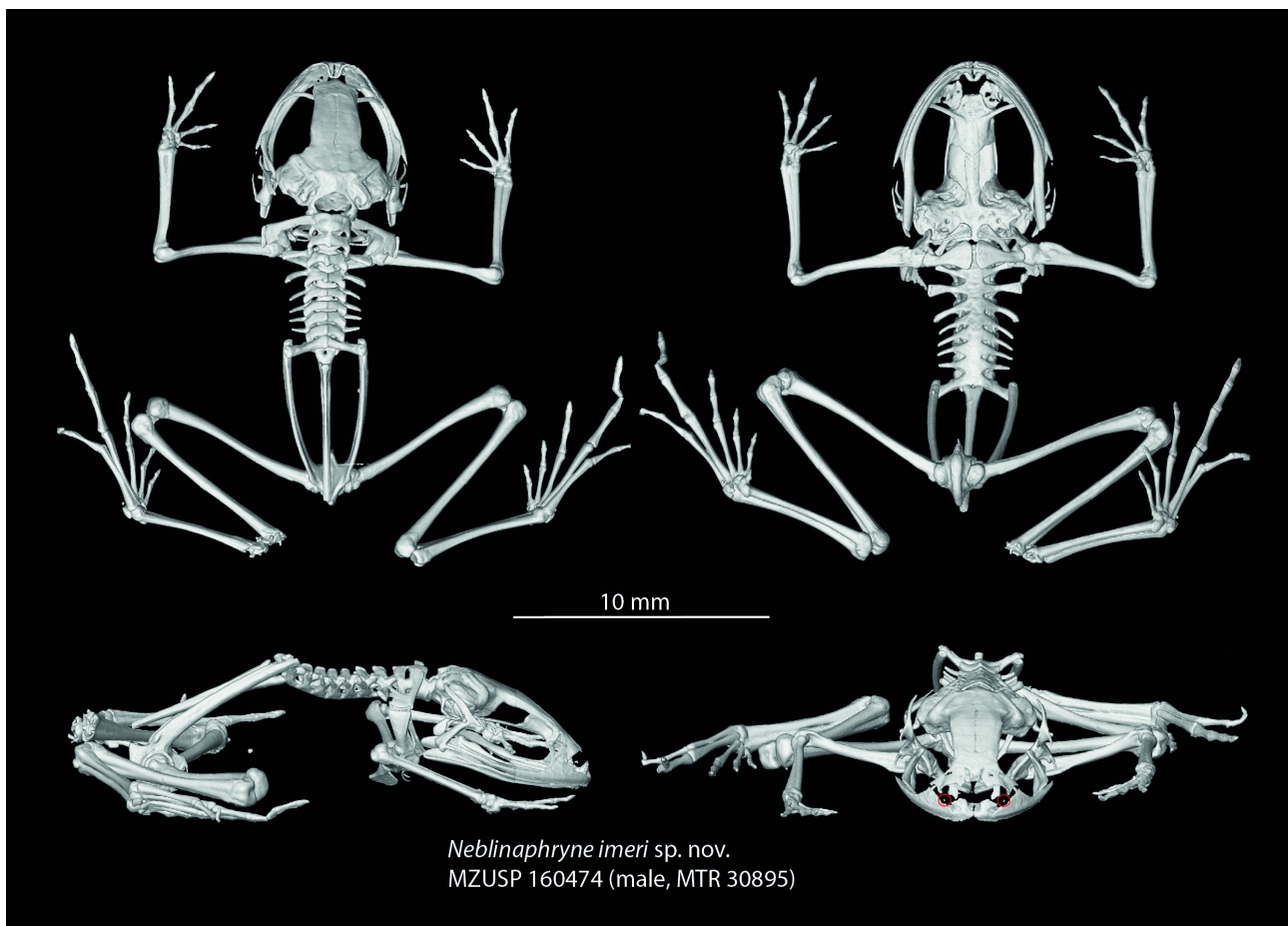


**FIGURE 6.** Volume renderings of a male paratype (MZUSP 160474 / MTR 30895) in dorsal, ventral, lateral, and frontal views. Minuscule septomaxillae are indicated by red circles in the frontal view.

**Coloration of holotype in life.** Dorsum reddish brown with irregular dark brown blotches and small white dots. Interorbital region with dark brown bar delimited anteriorly by cream line. Canthus rostralis, tip of snout, lips, and supratympanic folds with dark brown blotches and a few white dots. Coloration of flanks forming series of oblique stripes delimited by grayish lines, anteriorly dark brown, gray in middle, and posteriorly with oblique dark brown lateral stripe. Axillary and inguinal regions bright orange. Throat, belly and ventral surface of legs dark gray with many small white spots, with diffuse bright orange blotches posteriorly. Dorsal surface of arms and legs same as dorsum but with dark brown blotches forming transverse bands. Inner surface of shank and feet bright orange. Iris copper with dark brown vertical bar on its upper and lower portions, only reaching the pupil on the lower part.

**Variation.** Morphometric variation is summarized in Table 1. Females are larger than males (SVL 19.2–20.1 mm in females and 14.2–17.2 mm in males). The coloration is highly variable, especially the distribution of dark



brown blotches and the extent of orange blotches. Only the dark brown supratympanic blotch and the interorbital bar are found in all the specimens. Females have fewer dark brown blotches, but the variation of bright orange marks does not seem to be related to sex. The orange marks vary from tiny blotches in the inguinal regions and blotches on shanks (MZUSP 160480/MTR 31003) to being extensively distributed on the throat and belly and the entirety of the ventral sides of the arms and thighs, axillae, inguinal regions, and shanks (MZUSP 160472/MTR 30864). One female (MZUSP 160473/MTR 30892) has wide, well-defined, light brown dorsolateral lines. Two males (MZUSP 160477 / MTR 30988, MZUSP 160480 / MTR 31003) have less conspicuous dorsolateral lines. A single male (MZUSP 160478/MTR 30990) has many dark brown blotches on the belly.

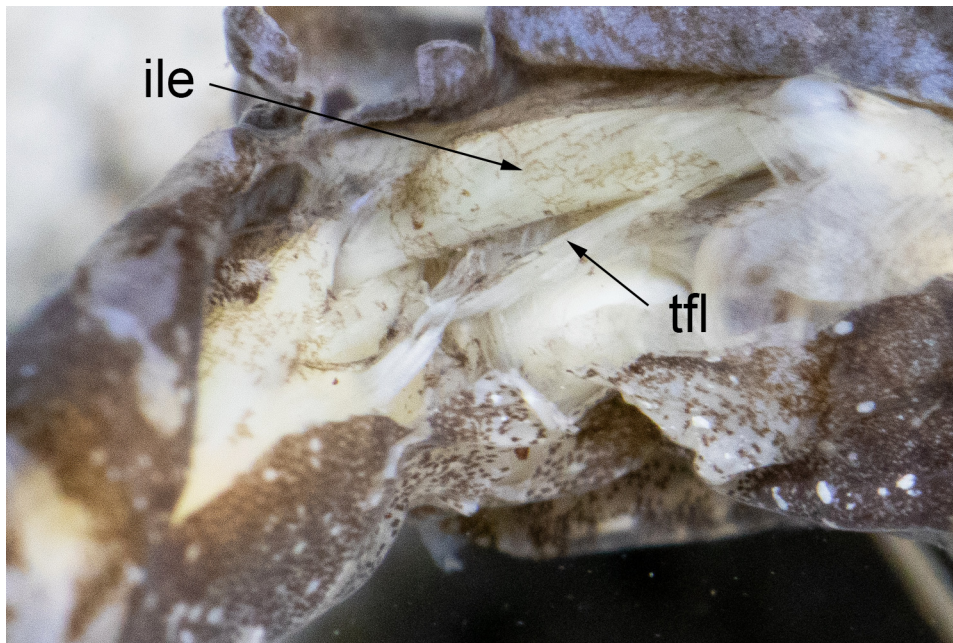


**FIGURE 7.** Photograph of the posterior side of the thigh of *Neblinaphryne imeri* **sp. nov.** (paratype male, MZUSP 160477 / MTR 30988) showing the *m. iliacus externus* (ile) and the *m. tensor fasciae latae* (tfl).

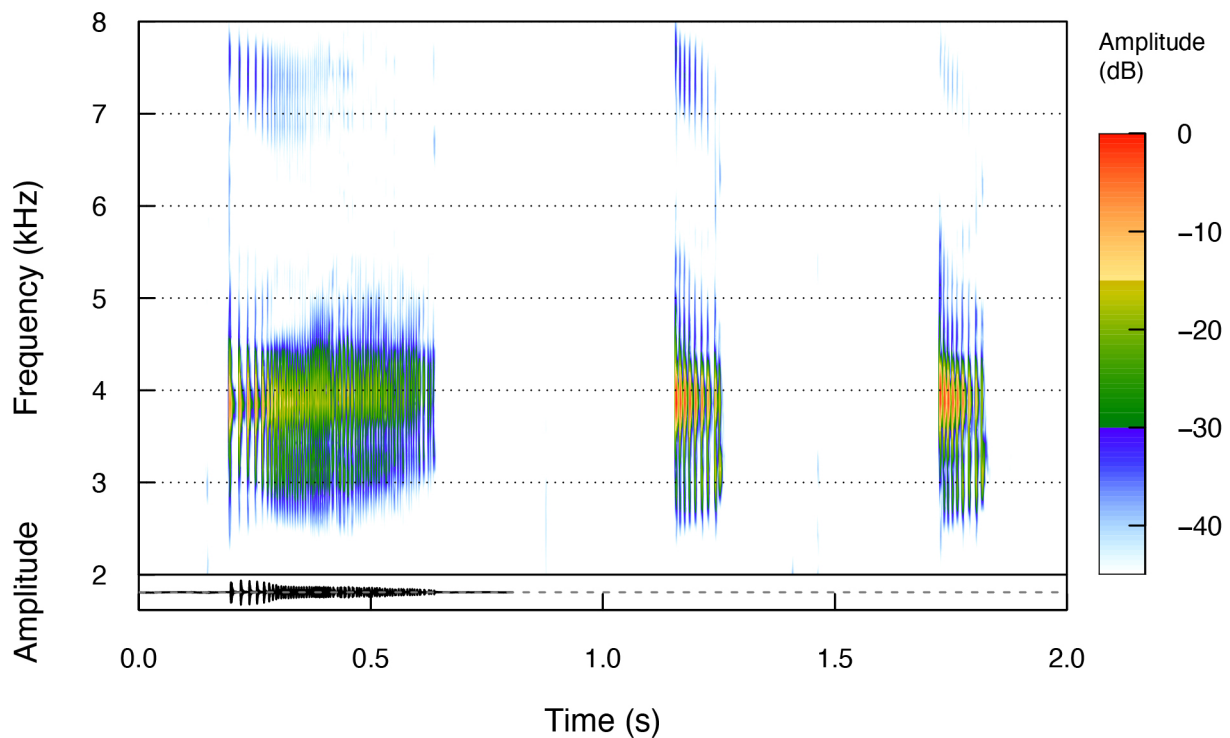


**FIGURE 8.** Spectrogram and oscillogram of the advertisement call of *Neblinaphryne imeri* **sp. nov.** (holotype MZUSP 160479/ MTR 30991) consisting of one Type 1 note and two Type 2 notes.

**Osteology.** The following description is based on the skeleton examined by volume rendering of MZUSP 160474 (male paratype, field number MTR 30895; Fig. 6). Two additional specimens were examined and agree with this description. The osteology is very similar to *N. mayeri* that has been extensively described by Fouquet *et al.* (2024). Therefore, we only mention the observed differences below: Cranium larger than long; palatine slightly curved and expanding towards sphenethmoid; alary processes of premaxilla with omega-shaped ridge posterodorsally; pterygoid long, reaching neopalatine anteriorly; quadratojugal very short; angulosplenial only slightly sigmoid; neural arches of presacrals well developed, bearing large, projecting neural crests on presacrals III–IV only; calcanea and astragali partly fused with only a narrow gap medially; absence of fabella sesamoid (Abdala *et al.* 2019).

**Osteological variation (Appendix 3).** The osteological features of two additional specimens have been examined (MZUSP 160473/ MTR 30892; MZUSP 160478 / MTR 30990). We did not observe any noteworthy deviation from MZUSP 160474 (MTR 30895).

**Advertisement call.** The call consists of two types of notes (Fig. 8; Table 2). Type 1 notes are long (414–592 ms) series of pulses (31–70 pulses) emitted at increasing rate (silence between pulses 15–34 at the beginning of the call vs 9–17 ms at the end of the call) within the note and downward frequency modulation (starting dominant frequency 3,349–3,957 Hz; ending dominant frequency 3,010–3,882 Hz). A harmonic structure is visible as high as ca. 13,000 Hz (not shown) with the most intense harmonics being ca. 7,000–7,500 and 9,500–10,000 Hz (not shown). Type 1 notes are often emitted alone, whereas series of 2–4 Type 2 notes are generally emitted after Type 1 notes. Type 2 notes have the same basic structure and dominant frequency (3,356–4,023 Hz) as Type 1 notes but are shorter (76–180 ms) and have fewer pulses (7–20).

**TABLE 2.** Acoustic variables across four recorded males (one measurement of each variable per recorded male).

Variable	Mean±s.d. (Min–Max)
Call length (ms)	1809 ± 128.8 (1689–2001)
Note length 1 (ms)	592 ± 81.9 (414–592)
Note length 2 (ms)	142.5 ± 44.6 (76–180)
Silence between Type 1 and 1 <sup>st</sup> Type 2 notes (ms)	475 ± 56.9 (431–558)
Silence between 1 <sup>st</sup> and 2 <sup>nd</sup> Type 2 notes (ms)	455 ± 70.9 (400–570)
Number of pulses/Type 1 notes	70 ± 17.5 (31–70)
Number of pulses/Type 2 notes	11 ± 5.8 (7–20)
Number of interpulse silence start Type 1 notes (ms)	18 ± 8.5 (15–34)
Number of interpulse silence end Type 1 notes (ms)	9 ± 3.9 (9–17)
Fundamental start Type 1 (Hz)	2843 ± 250 (2564–3150)
Dominant start Type 1 (Hz)	3957 ± 265 (3349–3957)
Fundamental end Type 1 (Hz)	2371 ± 409 (2371–3144)
Dominant end Type 1 (Hz)	3324 ± 393 (3010–3882)
Delta Dominant frequency Type 1 (Hz)	633 ± 358 (-72–723)
Dominant frequency Type 2 (Hz)	3799 ± 286 (3356–4023)

**Comparison with other species.** *Neblinaphryne imeri* **sp. nov.** is distinguished from *N. mayeri* (in parentheses) by the following traits: (1) coloration characterized by dark brown blotches scattered on dorsal surface of the body, whitish dots and orange marks on the inguinal region, inner surface of arms, legs and venter (almost uniformly brown on dorsum, without white dots and orange marks); (2) one cream colored (white in life) tubercle on each eyelid (absent); (3) prominent white-tipped, humeral tubercle present (absent); (4) palatine slightly curved, expanding towards sphenethmoid (straight, tapering towards sphenethmoid); (5) pterygoid long, reaching palatine anteriorly (not reaching); (6) alary processes of premaxilla with omega-shaped ridge posterodorsally (without ridge); (7) presacral neural arches bearing large, projecting neural crests on presacrals III–IV (present on presacrals II–IV); (8) calcanea and astragali partly fused with only a narrow gap medially (large gap); (9) fabella sesamoid absent (fabella sesamoid present, large).

*Neblinaphryne imeri* **sp. nov.** can be distinguished from all the brachycephaloids examined by Fouquet *et al.* (2024; in parentheses) except *N. mayeri* by its pointed terminal phalanges (T-shaped) and minuscule septomaxillae (large). It can be further distinguished from the four other brachycephaloid lineages occurring in



Pantepui—*Adelophryne* (Eleutherodactylidae, Phyzelaphryninae), *Pristimantis* (Strabomantidae, Pristimantinae), *Ceuthomantis* (Ceuthomantidae), and *Dischidodactylus* (incertae sedis)—as follows (character states of other taxa in parentheses): from *Adelophryne* by its fully developed fingers and toes (reduced Finger IV), with mucronate tips on Fingers II–IV and Toes II–IV only (most digits with mucronate tips), and without a lateral groove (with groove); lack of vomerine teeth (present), and from *Ceuthomantis*, *Pristimantis*, and *Dischidodactylus* by its mucronate tips on Fingers II–IV and Toes II–IV (rounded) and *m. tensor fasciae latae* originating anteriorly on the iliac shaft (posterior or middle). It can be further distinguished from *Ceuthomantis* and *Dischidodactylus* by its *m. iliacus externus* originating anteriorly on the iliac shaft (vs. originating on the posterior half or three-fourths of the iliac shaft) and from *Dischidodactylus* by the lack of vomerine teeth (present).

**Distribution (Fig. 1).** *Neblinaphryne imeri* **sp. nov.** is known only from the type locality, in the Serra do Imeri, Parque Nacional do Pico da Neblina, Santa Isabel do Rio Negro, Amazonas state, Brazil. Based on the spatial distribution of calling males, the species seems quite abundant in both the open vegetation covering the top of the massif, at elevations between 1,800 and 1,940 m, and in the adjacent mountain forests. Below 1,800 m the species becomes rarer, and no calling males were heard at 1,700 m.

**Natural history.** In both open and forested habitats *Neblinaphryne imeri* is very difficult to locate and capture. Females were opportunistically found when searching for calling males (e.g. MZUSP 160472/MTR 30864), suggesting that they were reproductively active, which is corroborated by large oocytes (oviduct expanded and oocytes white, two oocytes measured 1.5–1.7 mm diameter in MZUSP 160472, other smaller oocytes not counted to avoid damaging the specimen), possibly attracted by the calling male. In open habitat, the species calls beneath herbaceous vegetation or in dry leaves and stems of rosette-forming plants, such as giant bromeliads. In forested habitat, individuals call from deep inside the layers of moss. The holotype MZUSP 160479 (MTR 30991) was calling from inside a theraphosid (tarantula) burrow. Based on the calling activity, *Neblinaphryne imeri* **sp. nov.** is diurnal, vocalizing throughout the day but with peak activity during the first hours of light in the morning and the end of day until the first hour of darkness.

## Discussion

Pantepui probably still hides many undocumented species, notably in the poorly explored massifs scattered across the region and along the slopes of massifs, even the ones whose highest parts have been extensively documented. To our knowledge, this is the first scientific exploration of the Imeri massif and it unsurprisingly led to the discovery of several undescribed anuran species, including the one described herein.

*Neblinaphryne imeri* is the second species of this recently described genus and family. With *N. mayeri*, they represent a singular lineage that diverged ca. 55 Ma from its closest relatives and is seemingly endemic to the southern part of Pantepui, like *Metaphryniscus*, *Dischidodactylus*, and *Minyobates* (Lynch 1979; Myers 1987; Señaris *et al.* 1994), while other genera endemic to the region, such as *Nesorohyla* and *Oreophrynella*, are restricted to the eastern part (Kok *et al.* 2018; Pinheiro *et al.* 2019). Moreover, the genera that have been documented throughout the region, such as *Anomaloglossus* (Vacher *et al.* 2024) and *Stefania* (Kok *et al.* 2017), generally display very ancient divergences across Pantepui. These patterns highlight the fact that the most distant massifs within Pantepui have a long history of isolation. However, adjacent massifs can harbor recently formed species (Kok *et al.* 2018). In the case of the two species of *Neblinaphryne*, which are putatively isolated by a minimum of 20 km of lowlands, the genetic distance of almost 6% in 16S can be considered relatively high, especially when compared to the low genetic distances usually observed among tepui summit taxa (Kok *et al.* 2012) that are more topographically isolated than this new species. However, the region is so poorly documented that each of these two species could have closer relatives that remain to be discovered.

The osteology of the two species is remarkably conserved, and this second species confirmed that relict septomaxillae and pointed terminal phalanges are synapomorphies of *Neblinaphryne*. However, their external morphologies are remarkably distinct. *Neblinaphryne mayeri* has very inconspicuous dorsal and ventral coloration, although diffuse yellow pigmentation can be present in variable degrees, while *N. imeri* harbors striking dorsal patterns and conspicuous bright orange inguinal and ventral blotches. *Neblinaphryne mayeri* and *N. imeri* inhabit different elevations and habitats: *N. mayeri* is found in open vegetation at 2,000–2,995 m elevation and is most often found under rocks; *N. imeri* lives at 1,700–2,000 m elevation, typically under giant bromeliads in open habitats,

or inside moss mats within the mountain forest. These ecological differences could explain the distinct external morphology, while osteological features are more conserved.

## Acknowledgments

We thank Generals Sinclair James Mayer, Achilles Furlan Neto, Andrelucio Couto, Cláudio Henrique Plácido, Colonel Márcio Weber de Menezes, Majors Flávio Lacerda and Kleber Yañez, Captains Jefferson Fagundes and Jorge Leandro, and all personnel of the Brazilian Army involved in planning and providing logistical support during the expedition to Serra do Imeri. We also warmly thank Eloisa Cabral (SISDIA) and Paulo Muzy from the University of São Paulo for support and our field colleagues Lúcia Lohmann and Rafaela Forzza (botany), Alexandre Percequillo and Ana Paula Carmignotto (mammals), Luis Fábio Silveira and Igor Alvarenga (ornithology), Bruno Fermino (parasitology) and the journalists Herton Escobar, Paulina Chamorro, and Andre Dib for help in the field. Phillip Lenktaitis and Enio Mattos helped with scanning specimens, Manuel Antunes Júnior and Juliana N. Tanaka provided assistance at IB-USP with tissue collection and in the molecular laboratory, and Aline Benetti and Karolina Reis provided collection support at MZUSP. FUNAI and ICMBio provided the licenses for the expedition. Fundação de Amparo à Pesquisa do Estado de São Paulo (FAPESP 2011/50146-6, 2018/15425-0, 2022/01213-7) and Conselho Nacional de Desenvolvimento Científico e Tecnológico (CNPq 301778/2015-9, 314480/2021-8) provided financial support. AF acknowledges support from “Investissement d’Avenir” grant managed by the Agence Nationale de la Recherche (CEBA, ref. ANR-10-LABX-25-01).

## References

- Abdala, V., Vera, M.C., Amador, L.I., Fontanarrosa, G., Fratani, J. & Ponssa, M.L. (2019) Sesamoids in tetrapods: the origin of new skeletal morphologies. *Biological Reviews*, 94, 2011–2032.  
<https://doi.org/10.1111/brv.12546>
- Berry, P.E. & Riina, R. (2005) Insights into the diversity of the Pantepui flora and the biogeographic complexity of the Guayana Shield. *Biologiske Skrifter*, 55, 145–167.
- Cervino, N.G., Elias-Costa, A.J., Pereyra, M.O. & Faivovich, J. (2021) A closer look at pupil diversity and evolution in frogs and toads. *Proceedings of the Royal Society B*, 288 (1957), 20211402.  
<https://doi.org/10.1098/rspb.2021.1402>
- Duellman, W.E. & Lehr, E. (2009) *Terrestrial-breeding frogs (Strabomantidae) in Peru*. Natur und Tier Verlag GmbH, Münster, 384 pp.
- Dunlap, D.G. (1960) The comparative myology of the pelvic appendage in the Salientia. *Journal of Morphology*, 106, 1–76.  
<https://doi.org/10.1002/jmor.1051060102>
- Felsenstein, J. (1985) Confidence limits on phylogenies: an approach using the bootstrap. *Evolution*, 39 (4), 783–791.  
<https://doi.org/10.1111/j.1558-5646.1985.tb00420.x>
- Fouquet, A., Gilles, A., Vences, M., Marty, C., Blanc, M. & Gemmell, N.J. (2007) Underestimation of species richness in Neotropical frogs revealed by mtDNA analyses. *PLoS ONE*, 2 (10), e1109.  
<https://doi.org/10.1371/journal.pone.0001109>
- Fouquet, A., Kok, P.J.R., Recoder, R.S., Prates, I., Camacho, A., Marques-Souza, S., Ghellere, J.M., McDiarmid, R.W. & Rodrigues, M.T. (2024) Relicts in the mist: Two new frog families, genera and species highlight the role of Pantepui as a biodiversity museum throughout the Cenozoic. *Molecular Phylogenetic & Evolution*, 191, 107971.  
<https://doi.org/10.1016/j.ympev.2023.107971>
- Heinicke, M.P., Duellman, W.E., Trueb, L., Means, D.B., MacCulloch, R.D. & Hedges, S.B. (2009) A new frog family (Anura: Terrarana) from South America and an expanded direct-developing clade revealed by molecular phylogeny. *Zootaxa*, 2211 (1), 1–35.  
<https://doi.org/10.11646/zootaxa.2211.1.1>
- Kalyaanamoorthy, S., Minh, B.Q., Wong, T.K.F., von Haeseler, A. & Jermin, L.S. (2017) ModelFinder: Fast model selection for accurate phylogenetic estimates. *Nature Methods*, 14, 587–589.  
<https://doi.org/10.1038/nmeth.4285>
- Katoh, K. & Standley, D.M. (2013) MAFFT Multiple sequence alignment software Version 7: Improvements in performance and usability. *Molecular Biology & Evolution*, 30, 772–780.  
<https://doi.org/10.1093/molbev/mst010>
- Köhler, J., Jansen, M., Rodriguez, A., Kok, P.J., Toledo, L.F., Emmrich, M., Glaw, F., Haddad, C.F.B., Rödel, M.-O. & Vences, M. (2017) The use of bioacoustics in anuran taxonomy: theory, terminology, methods and recommendations for best



- practice. *Zootaxa*, 4251 (1), 1–124.  
<https://doi.org/10.11646/zootaxa.4251.1.1>
- Kok, P.J.R. (2005) A new genus and species of gymnophthalmid lizard (Squamata: Gymnophthalmidae) from Kaieteur National Park, Guyana. *Bulletin de l'Institut Royal des Sciences Naturelles de Belgique Biologie*, 75, 35–45.
- Kok, P.J.R. (2009) Lizard in the clouds: a new highland genus and species of Gymnophthalmidae (Reptilia: Squamata) from Maringma tepui, western Guyana. *Zootaxa*, 1992, 53–67.  
<https://doi.org/10.11646/zootaxa.1992.1.4>
- Kok, P.J.R. (2013) *Islands in the Sky: Species Diversity, Evolutionary History, and Patterns of Endemism of the Pantepui Herpetofauna*. PhD thesis, Leiden University, Leiden. [unknown pagination]
- Kok, P.J.R. (2015) A new species of the Pantepui endemic genus *Riolama* (Squamata: Gymnophthalmidae) from the summit of Murisipán-tepui, with the erection of a new gymnophthalmid subfamily. *Zoological Journal of the Linnean Society*, 174 (3), 500–518.  
<https://doi.org/10.1111/zoj.12241>
- Kok, P.J.R., MacCulloch, R.D., Means, D.B., Roelants, K., Van Bocxlaer, I. & Bossuyt, F. (2012) Low genetic diversity in tepui summit vertebrates. *Current Biology*, 22 (15), R589–90.  
<https://doi.org/10.1016/j.cub.2012.06.034>
- Kok, P.J.R., Ratz, S., MacCulloch, R.D., Lathrop, A., Dezfoulian, R., Aubret, F. & Means, D.B. (2018) Historical biogeography of the palaeoendemic toad genus *Oreophrynella* (Amphibia: Bufonidae) sheds a new light on the origin of the Pantepui endemic terrestrial biota. *Journal of Biogeography*, 45 (1), 26–36.  
<https://doi.org/10.1111/jbi.13093>
- Kok, P.J.R., Russo, V.G., Ratz, S., Means, D.B., MacCulloch, R.D., Lathrop, A., Aubret, F. & Bossuyt, F. (2017) Evolution in the South American ‘Lost World’: insights from multilocus phylogeography of stefanias (Anura, Hemiphractidae, *Stefania*). *Journal of Biogeography*, 44, 170–181.  
<https://doi.org/10.1111/jbi.12860>
- Kok, P.J.R., van Doorn, L. & Dezfoulian, R. (2019) Predation by non-bioluminescent firefly larvae on a tepui-summit endemic toad. *Current Biology*, 29 (22), R1170–R1171.  
<https://doi.org/10.1016/j.cub.2019.10.001>
- Kok, P.J.R. & Means, D.B. (2023) Hiding in the mists: Molecular phylogenetic position and description of a new genus and species of snake (Dipsadidae: Xenodontinae) from the remote cloud forest of the Lost World. *Zoological Journal of the Linnean Society*, zlad082. [published online]  
<https://doi.org/10.1093/zoolinnean/zlad082>
- Leite, Y.L., Kok, P.J.R. & Weksler, M. (2015) Evolutionary affinities of the ‘Lost World’ mouse suggest a late Pliocene connection between the Guiana and Brazilian shields. *Journal of Biogeography*, 42 (4), 706–715.  
<https://doi.org/10.1111/jbi.12461>
- Lynch, J.D. (1979) A new genus for *Elosia duidensis* Rivero (Amphibia, Leptodactylidae) from southern Venezuela. *American Museum Novitates*, 2680, 1–8
- Lynch, J.D. & Duellman, W.E. (1997) Frogs of the genus *Eleutherodactylus* in western Ecuador. *University of Kansas Special Publication*, 23, 1–236.  
<https://doi.org/10.5962/bhl.title.7951>
- Mayr, E. & Phelps, W.H. (1967) The origin of the bird fauna of the south Venezuelan highlands. *Bulletin of the American Museum of Natural History*, 136, 273–327.
- Minh, B.Q., Schmidt, H.A., Chernomor, O., Schrempf, D., Woodhams, M.D., von Haeseler, A. & Lanfear, R. (2020) IQ-TREE 2: New models and efficient methods for phylogenetic inference in the genomic era. *Molecular Biology & Evolution*, 37, 1530–1534.  
<https://doi.org/10.1093/molbev/msaa015>
- Myers, C.W. (1987) New generic names from some neotropical poison frogs (Dendrobatidae). *Papéis Avulsos de Zoologia*, 36, 301–306.  
<https://doi.org/10.11606/0031-1049.1983.36.p301-306>
- Myers, C.W. & Donnelly, M.A. (2001) Herpetofauna of the Yutajé-Corocoro Massif, Venezuela: second report from the Robert G. Goelet American Museum - Terramar Expedition to the Northwestern Tepuis. *Bulletin of the American Museum of Natural History*, 261, 1–85.  
[https://doi.org/10.1206/0003-0090\(2001\)261<0001:HOTYCM>2.0.CO;2](https://doi.org/10.1206/0003-0090(2001)261<0001:HOTYCM>2.0.CO;2)
- Ortiz, D.A., Hoskin, C.J., Werneck, F.P., Réjaud, A., Manzi, S., Ron, S.R. & Fouquet, A. (2022) Historical biogeography of a diverse tree frog clade highlights a key role of Miocene landscape changes on Amazonian diversification. *Organisms Diversity and Evolution*, 23 (2), 395–414.  
<https://doi.org/10.1007/s13127-022-00588-2>
- Ospina-Sarria, J.J. & Grant, T. (2022) New phenotypic synapomorphies delimit three molecular-based clades of New World direct-developing frogs (Amphibia: Anura: Brachycephaloidea). *Zoological Journal of the Linnean Society*, 195 (3), 976–994.  
<https://doi.org/10.1093/zoolinnean/zlab071>
- Pellegrino, K.C.M., Brunes, T.O., Souza, S.M., Laguna, M.M., Avila-Pires, T.C.S., Hoogmoed, M.S. & Rodrigues, M.T. (2018)

- On the distinctiveness of *Amapasaurus*, its relationship with *Loxopholis* Cope 1869, and description of a new genus for *L. guianensis* and *L. hoogmoedi* (Gymnophthalmoidea/Ecpleopodini: Squamata). *Zootaxa*, 4441 (2), 332–346.  
<https://doi.org/10.11646/zootaxa.4441.2.8>
- Pinheiro, P.D., Kok, P.J.R., Noonan, B.P., Means, D.B., Haddad, C.F. & Faivovich, J. (2019) A new genus of Cophomantini, with comments on the taxonomic status of *Boana liliae* (Anura: Hylidae). *Zoological Journal of the Linnean Society*, 185 (1), 226–245.  
<https://doi.org/10.1093/zoolinnean/zly030>
- Recoder, R., Prates, I., Marques-Souza, S., Camacho, A., Nunes, P.M.S., Dal Vechio, F., Ghellere, J.M., McDiarmid, R.W. & Rodrigues, M.T. (2020) Lizards from the Lost World: two new species and evolutionary relationships of the Pantepui highland *Riolama* (Gymnophthalmidae). *Zoological Journal of the Linnean Society*, 190 (1), 271–297.  
<https://doi.org/10.1093/zoolinnean/zlz168>
- Rueden, C.T., Schindelin, J., Hiner, M.C., DeZonia, B.E., Walter, A.E., Arena, E.T. & Eliceiri, K.W. (2017) ImageJ2: ImageJ for the next generation of scientific image data. *BMC Bioinformatics*, 18.  
<https://doi.org/10.1186/s12859-017-1934-z>
- Rull, V., Montoya, E., Nogué, S., Safont, E. & Vegas-Vilarrúbia, T. (2019) Climatic and ecological history of Pantepui and surrounding areas. In: Rull, V., Montoya, E., Nogué, S., Safont, E. & Vegas-Vilarrúbia, T. (Eds.), *Biodiversity of Pantepui. The Pristine “Lost World” of the Neotropical Guiana Highlands*. Academic press, Cambridge, pp. 33–54.  
<https://doi.org/10.1016/B978-0-12-815591-2.00002-1>
- Rull, V. & Vegas-Vilarrúbia, T. (2020) The Pantepui “Lost World”: towards a biogeographical, ecological and evolutionary synthesis of a pristine Neotropical sky-island archipelago. In: Rull, V. & Carnaval, A.C.Q. (Eds.), *Neotropical Diversification: Patterns and Processes*. Springer, Cham, pp. 369–413.  
[https://doi.org/10.1007/978-3-030-31167-4\\_15](https://doi.org/10.1007/978-3-030-31167-4_15)
- Santos, J.C., Coloma, L.A., Summers, K., Caldwell, J.P., Ree, R. & Cannatella, D.C. (2009) Amazonian amphibian diversity is primarily derived from later Miocene Andean lineages. *PLoS Biology*, 7, 448–461.  
<https://doi.org/10.1371/journal.pbio.1000056>
- Señaris, J.C., Ayarzagüena, J. & Gorzula, S.J. (1994) Los sapos de la familia Bufonidae (Amphibia: Anura) de las tierras altas de la Guayan Venezolana: Descripción de un nuevo genero y tres especies. *Publicaciones de la Asociación de Amigos de Doñana*, 3, 1–37.
- Steyermark, J.A. (1986) Holstianthus, a new genus of Rubiaceae from the Guayana highland. *Annals of the Missouri Botanical Garden*, 73 (2), 495–497.  
<https://doi.org/10.2307/2399130>
- Vacher, J.-P., Kok, P.J.R., Rodrigues, M.T., Lima, A.P., Hrbek, T., Werneck, F.P., Manzi, S., Thébaud, C. & Fouquet, A. (2024) Diversification of terrestrial frogs within the Guiana Shield: from highlands to lowlands and successive loss and reacquisition of endotrophy in *Anomaloglossus* (Aromobatidae). *Molecular Phylogenetics & Evolution*, 192, 108008.  
<https://doi.org/10.1016/j.ympev.2023.108008>
- Vanzolini, P.E. & Williams, E.E. (1981) The vanishing refuge: a mechanism for ecogeographic speciation. *Papéis Avulsos de Zoologia*, 34 (23), 251–255.  
<https://doi.org/10.11606/0031-1049.1980.34.p251-255>



## APPENDIX 1. Primer details.

12S rDNA	L13	Forward	TTAGAAGAGGCAAGTCGTAACATGGTA	Feller and Hedges, 1998
	Titus I	Reverse	GGTGGCTGCTTTTAGGCC	Titus and Larson, 1996
16S rDNA	L2A	Forward	CCAAACGAGCCTAGTGATAGCTGGTT	Hedges, 1994
	H10	Reverse	TGATTACGCTACCTTTGCACGGT	Hedges, 1994
	AR	Forward	CGCCTGTTTATCAAAAACAT	Palumbi <i>et al.</i> , 1991
	BR	Reverse	CCGGTCTGAACTCAGATCACGT	Palumbi <i>et al.</i> , 1991
cytochrome oxidase c subunit 1	LCO1490	Forward	GGTCAACAAATCATAAAGATATTGG	Folmer <i>et al.</i> , 1994
	HCO2198	Reverse	TAAACTTCAGGGACCAAAAAATC	Folmer <i>et al.</i> , 1994

## APPENDIX 2. GenBank accession numbers and voucher information for the mitochondrial DNA sequences used for the phylogenetic analysis.

16S	COI	Genus	species	Voucher
<b>PP789109</b>	<b>PP788591</b>	<i>Neblinaphryne</i>	<i>imeri</i> <b>sp. nov.</b>	MTR30964
OR416190	OR416190	<i>Neblinaphryne</i>	<i>mayeri</i>	MTR40345
OR416189	OR416189	<i>Ceuthomantis</i>	<i>sp. Neblina</i>	MTR40261
OP476272	OP476272	<i>Pristimantis</i>	<i>koehleri</i>	SCF513
OP476213	OP476213	<i>Holoaden</i>	<i>luederwaldti</i>	AF1600
OP476225	OP476225	<i>Niceforonia</i>	<i>brunnea</i>	AF4820
OP476229	OP476229	<i>Diasporus</i>	<i>sp.</i>	AFJ215
OP476235	OP476235	<i>Adelophryne</i>	<i>gutturosa</i>	BPN3765
OP476227	OP476227	<i>Craugastor</i>	<i>raniformis</i>	AFJ202
MH492735	MH492735	<i>Ischnocnema</i>	<i>erythromera</i>	CFBH40985
MZ770744	MZ770744	<i>Brachycephalus</i>	<i>quiririensis</i>	?
MH492737	MH492737	<i>Ischnocnema</i>	<i>guentheri</i>	CFBH27440
MZ770752	MZ770752	<i>Ischnocnema</i>	<i>henselii</i>	?
OP476254	OP476254	<i>Strabomantis</i>	<i>sulcatus</i>	MTR36755
OP476219	OP476219	<i>Pristimantis</i>	<i>aff. pluvialis</i>	AF2764
OP476271	OP476271	<i>Pristimantis</i>	<i>skydmainos</i>	SCF381
OP815325	KP149091	<i>Tachiramantis</i>	<i>douglasi</i>	ICN60815/AJC3492
KY962393	KY962393	<i>Phyllobates</i>	<i>terribilis</i>	TG3732
MH571152	MH571152	<i>Pseudis</i>	<i>tocantins</i>	?
OP476258	OP476258	<i>Bryophryne</i>	<i>bustamantei</i>	MUBI14314
JF703234	JF703234	<i>Telmatobius</i>	<i>bolivianus</i>	MNCNDNA563
MH070027	MH070027	<i>Eupsophus</i>	<i>vertebralis</i>	ICMLH495
KT221614	KT221614	<i>Hylodes</i>	<i>meridionalis</i>	?
OP476212	OP476212	<i>Haddadus</i>	<i>binotatus</i>	AF1463
OP476222	OP476222	<i>Noblella</i>	<i>myrmecoides</i>	AF4468
JX564864	JX564864	<i>Eleutherodactylus</i>	<i>atkinsi</i>	MVZ241209
JX564870	JX564870	<i>Craugastor</i>	<i>augusti</i>	TNHC-GDC12606
JX564880	JX564880	<i>Odontophrynus</i>	<i>occidentalis</i>	MVZ145207
JX564866	JX564866	<i>Gastrotheca</i>	<i>pseustes</i>	TNHC62492
JX564869	JX564869	<i>Hyalinobatrachium</i>	<i>fleischmanni</i>	MVZ207146
OP476249	OP476249	<i>Phyzelaphryne</i>	<i>miriamae</i>	MTR19437
OP476247	OP476247	<i>Adelophryne</i>	<i>baturitensis</i>	MTR14012
MZ770742	MZ770742	<i>Brachycephalus</i>	<i>pulex</i>	?

.....continued on the next page

APPENDIX 2. (Continued)

16S	COI	Genus	species	Voucher
OP476257	OP476257	<i>Phynopus</i>	<i>horstpauli</i>	MUBI14219
OP476248	OP476248	<i>Oreobates</i>	<i>quixiensis</i>	MTR19385
OP476266	OP476266	<i>Pristimantis</i>	<i>lanthanites</i>	QCAZA19209
OP476260	OP476260	<i>Pristimantis</i>	<i>curtipes</i>	QCAZ3533
OP476255	OP476255	<i>Pristimantis</i>	<i>simonsii</i>	MUBI11407
OP476236	OP476236	<i>Pristimantis</i>	<i>moa</i>	ESTR2177
OP476215	OP476215	<i>Pristimantis</i>	<i>gutturalis</i>	AF2356
OP476262	OP476262	<i>Pristimantis</i>	aff. <i>malkini</i>	QCAZ51154
OP476259	OP476259	<i>Pristimantis</i>	<i>diadematus</i>	MUBI16183
OP476218	OP476218	<i>Pristimantis</i>	<i>espedeus</i>	AF2616
OP476268	OP476268	<i>Pristimantis</i>	<i>galdi</i>	QCAZA65032
OR416186	OR416186	<i>Caligophryne</i>	<i>doylei</i>	MTR40230
OP815323	OP787207	<i>Serranobatrachus</i>	<i>sanctaemartae</i>	ICN60807/ICN60811
JX564861	JX564861	<i>Cryptobatrachus</i>	<i>fuhrmanni</i>	TNHC-GDC-451
CM051072	CM051072	<i>Dendropsophus</i>	<i>ebraccatus</i>	?
JX564888	JX564888	<i>Pleurodema</i>	<i>thaul</i>	MVZ164826
JX564858	JX564858	<i>Ceratophrys</i>	<i>ornata</i>	?
JX564891	JX564891	<i>Rhinoderma</i>	<i>darwinii</i>	MVZ164829

APPENDIX 3. Volume renderings of two additional paratypes (MZUSP 160473 / MTR 30892; MZUSP 160478 / MTR 30990) in dorsal, ventral, lateral, and frontal views.

